



# HYBRID ALUMINUM MATRIX COMPOSITES PREPARED BY SPARK PLASMA SINTERING (SPS)

Zoltán Károly,<sup>[a]\*</sup> Csaba Balázsi,<sup>[b]</sup> Katalin Balázsi,<sup>[c]</sup> Attila Petrik,<sup>[b]</sup> János Lábár,<sup>[b]</sup> and Ayaj Dhar<sup>[d]</sup>

**Keywords:** Sintering; Al matrix composites; Graphene; Spark plasma sintering (SPS)

Aluminum Matrix composites have been intensively investigated over a long time due to their unique combination of beneficial properties including low density, high strength to weight ratio, increased hardness, advantageous tribology, corrosion resistance, etc. In the present work we studied the combined effect of various reinforcing phases including Al<sub>2</sub>O<sub>3</sub>, SiC, Si<sub>3</sub>N<sub>4</sub> and graphene on the aluminum matrix. The composites were fabricated by powder metallurgical method, in which the powder blend was rapidly sintered by spark plasma sintering. The main conclusion was that hybrid composite can perform better only if the development of porosity is eliminated by improving the wettability of the reinforcing particles.

\* Corresponding Authors

E-Mail: [karoly.zoltan@ttk.mta.hu](mailto:karoly.zoltan@ttk.mta.hu)

- [a] Institute of Materials and Environmental Chemistry, Research Centre for Natural Sciences HAS, Budapest, H-1025, Hungary  
 [b] Bay Zoltán Nonprofit Ltd. for Applied Research, H-1116 Budapest, Hungary  
 [c] Institute for Technical Physics and Material Science, Research Centre for Natural Sciences HAS, Budapest, H-1025, Hungary  
 [d] CSIR-National Physical Laboratory, New Delhi 110 012, India

## Introduction

Aluminum alloys has long been investigated for structural purposes. Their beneficial properties including low density, high thermal conductivity, high strength, corrosion resistance and toughness can be harnessed especially in the automotive and aeronautics industry due to the substantial weight reduction. The main obstacle of their tribological application is the low hardness and poor wear behavior. There are two main approaches to overcome these problems: (i) reducing the grain size of the metal matrix, (ii) or as more widespread method is the incorporation of hard reinforcing phases such as particles, whiskers or fibers into the aluminum matrix. The aluminum matrix composites with ceramic particles and fibers exhibited improved properties over monolithic aluminum alloys in terms of strength, wear resistance and yield. For reinforcing phase Si<sub>3</sub>N<sub>4</sub>, Al<sub>2</sub>O<sub>3</sub>, SiC, B<sub>4</sub>C, TiC and graphite particles are most frequently used.<sup>1</sup> The commonly used micron-sized reinforcing phases, however, considerably decrease the ductility of the matrix. It was found that strength can be increased without the decrease in the ductility in case of nanosized reinforcing phases.<sup>2</sup> Moreover, at the same volume ratio higher strengthening is achieved than micrometer counterparts.<sup>3</sup> The big challenge for nanosized reinforcing particles is their homogeneous dispersion within the matrix.

The effect of the various reinforcing phases has been widely studied, however, recent studies have focused on hybrid reinforcing when several type of reinforcing phases are incorporated in the matrix. In this way strength, young modulus and as well as reduction in the thermal expansion could be improved even more.<sup>4</sup> An interesting approach of

hybrid reinforcing is the dispersion of graphite particles beyond hard ceramic particles. The graphite particles improve the malleability of the matrix, while other valuable properties can be retained. This approach is especially advantageous in tribological applications as the graphite increases the resistance to seizure, while the composite has substantial strength due to other reinforcing phases.<sup>5-6</sup>

Substitution of graphite with graphene is also very promising. Beyond excellent electric, thermal and optical properties, graphene possesses outstanding mechanical properties, too. The flawless graphene is currently the strongest material with a Young modulus ( $E$ ) of 0.5-1 TPa and tensile strength ( $\sigma_{\text{int}}$ ) of 130 GPa.<sup>7</sup> There have been several trials to harness these properties in various composites incorporating 0.5-3 wt. % graphene. True graphene is currently prepared by epitaxial growing or other time-consuming and costly method with low production rate. It is much easier to prepare so-called multilayer graphene nanosheets (MLG) that consist of several or even several tens of graphene layers. These MLG are available as powder and their incorporation in the matrix is reported to improve the overall mechanical properties also.<sup>8-9</sup>

In the present work we investigated hybrid aluminum composites, in which beyond ceramic particles multilayer graphene nanosheets were also added. As a comparison, purely ceramic reinforced composites were also examined.

The two most widespread methods of composite production are the powder metallurgy and the casting (pressure and mixture casting). During production of ceramic reinforced aluminum composites homogenous dispersion of the reinforcing additives in the matrix is a significant unresolved problem. Nanosized ceramic particles are rather difficult to disperse in the aluminum matrix for two reasons: 1) the high viscosity of the molten aluminum; 2) the bad wettability of the ceramic by the aluminum melt. Mechanical mixing usually applied in case of micrometer sized powders is not suitable for nanosized counterparts because of the high surface to volume ratio that give rise to rapid agglomeration. One approach to circumvent this problem is the high energy milling during powder metallurgy.

Spark plasma sintering, a recently developed method has been increasingly applied both in powder metallurgy and in ceramic preparation as well.<sup>10</sup> Main advantage of this method over others is the much faster sintering at lower temperatures that makes possible to avoid the harmful grain coarsening and the unwanted reactions among the different phases.<sup>11</sup> The characteristics of this technology are the fast heating rate, the effective size reduction and the clean grain surface due to the plethora of microdischarges among the grains.

## Experimental

The starting powders used in these experiments were aluminum, SiC, Si<sub>3</sub>N<sub>4</sub>, Al<sub>2</sub>O<sub>3</sub> and graphene. Major characteristics (particle size, phase composition, etc.) of starting materials are listed in Table 1. Multilayer graphene (MLG) was prepared by milling synthetic graphite (Aldrich) in ethanol using a highly efficient attritor mill (Union Process, type 01-HD/HDDM) equipped with zirconia agitator delta discs and zirconia grinding media in a 750 ml silicon nitride tank. The milling process has been performed with high rotation speed, 4000 rpm until 10 h. The milled product was dried and sieved with a filter with a mesh size of 325. According to analysis the mean thickness of the crystallites was 13.7 nm, which is equivalent to ca.40 graphene layers.<sup>12</sup>

The aluminum was mixed with various reinforcing phases in different proportions. In the present work three of such composite compositions are discussed. The compositions of these experiments are as follows:

Exp. 1.: 70 wt.% Al + 30 wt.% Al<sub>2</sub>O<sub>3</sub>

Exp. 2.: 50 wt.% Al + 15 wt.% Al<sub>2</sub>O<sub>3</sub>+ 35 wt.% SiC

Exp. 3.: 30 wt.% Al + 50 wt.% Al<sub>2</sub>O<sub>3</sub>+ 10 wt.% SiC + 5 wt.% Si<sub>3</sub>N<sub>4</sub> + 5 wt.% graphene

The powders were mixed and homogenized also in an attritor mill in ethanol at 600 rpm until 1 h.

The obtained mixtures were then sintered to discs of 2 cm in diameter by spark plasma sintering machine (HD P5, FCT GmbH). A chamber pressure of 1 mbar was maintained during consolidation. The powders were uniaxially compressed throughout the sintering process with 50 MPa. Sintering was performed for 10 minutes at 600 °C using 100 °C heating rate. Temperature was continuously measured by thermocouples inserted to the graphite die. Linear reduction of the powder compacts was monitored on line by measuring the relative displacement of the graphite punch.

The density of the sintered materials was measured by Archimedes method. The hardness was measured using Vickers indentation method at loads of 3 N. Scanning electron microscopy (LEO 1540 XB FESEM) was used for the characterization of the obtained microstructure. Phase analysis of powders and sintered discs was performed by X-ray powder diffraction (XRD, Philips PW 1050) using Cu K $\alpha$  radiation.

**Table 1.** Main characteristics of the starting materials

Precursors	Source	Powder particle size, $\mu\text{m}$	Impurities (wt.%)
Aluminum		1-3	Fe+Si<0.2
Al <sub>2</sub> O <sub>3</sub>	ALMATIS, CT 3000LS SG	0.5	< 0.2
SiC	H.C. Stark, Grade UF-25	0.4	O <sub>2</sub> – 1.8
Si <sub>3</sub> N <sub>4</sub>	UBE America Inc., SN-ESP	0.5	O <sub>2</sub> - 2 C – 0.2

## Results

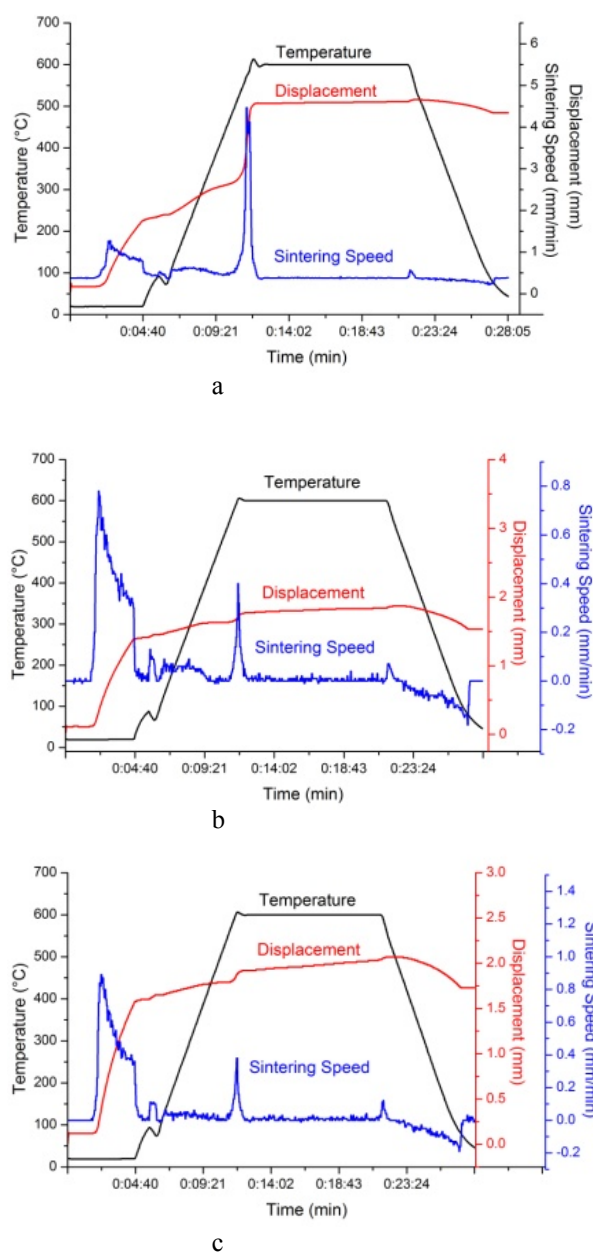
Figure 1.a-c show the sintering curves employed in the particular experiments including the temperature, the shrinkage as well as the rate of shrinkage as the function of the treatment time. The first peak of rate of shrinkage corresponds to the compaction of the powder on the effect of the applied compressive force. The peak around at 600 °C indicates, however, the starting of sintering. The highest overall shrinkage was observed in Experiment 1. This could be predicted taking into account the considerably high aluminum content of its starting composition. After 10 min of sintering further reduction could not be observed, while in the case of the other Experiments it seemingly did not finish that implies an incomplete sintering. It is confirmed by density values listed in Table 2. In Experiment 1 we achieved a 94 % theoretical density after consolidation, while that remained much smaller in the other experiments. The smaller theoretical density is in line with the findings<sup>3</sup> that increasing proportion of ceramic particles raise the porosity and the much less values of the obtained density agree with the theoretical ones. This is because the compressibility of the hard ceramic particles in a ductile matrix becomes difficult. The situation gets worse in case of nanosized reinforcing particles. The nanosized particles tend to agglomerate and create a network. It is interesting that usually higher density can be achieved using micron sized reinforcing particles because of their better compressibility and their smaller surface to volume ratio. Graphite as solid lubricant is considered to promote the relative motion and arrangement of the particles in the matrix material resulting in higher density.<sup>6</sup> Accordingly, in Experiment 3 containing graphene the apparent density became higher, however, in respect of theoretical density it gave a similar result as Experiment 2. It is probably due to the high content of reinforcing particles that surpass the aluminum matrix. The applied ceramic particles in all experiments were generally high in the hope that their effect on strength improvement would gradually increase with the proportion. Strength increasing mechanisms involve the increase in hardness due to grain refinement (Hall-Petch relationship), the hindering effect of the particles on dislocation motion as well as the accumulation of dislocations due to the different thermal expansion of the ceramic particles and the matrix material.<sup>3</sup>

**Table 2.** Density and hardness values of particular experiments

Experimental mixtures	Obtained density, g·cm <sup>-3</sup>	Theoretical density, %	Micro-hardness, GPa
No.1. 70 wt.% Al + 30 wt.% Al <sub>2</sub> O <sub>3</sub>	2.98	94	1.81
No.2. 50 wt.%Al + 15 wt.% Al <sub>2</sub> O <sub>3</sub> + 35 wt.% SiC	1.98	65	0.25
No.3. 30 wt.% Al + 50 wt.% Al <sub>2</sub> O <sub>3</sub> + 10 wt.% SiC + 5 wt.% Si <sub>3</sub> N <sub>4</sub> + 5 wt.% graphene	2.10	63	0.43

There is a great variation in microhardness values among samples of the particular experiments (Table 2). One suggests that with increasing proportion of ceramic particles hardness should be increased, too. In contrast, the highest value for hardness was obtained for the sample that contained reinforcing phases at the lowest proportion. The considerably smaller hardness of the other two experiments was probably due to the increased porosity. The increased hardness in experiment 3 compared to the 2<sup>nd</sup> one can most probably be attributed to the higher ceramic content of the former. Yet, it was not as high as expected because of the co-existence of higher porosity. The increased porosity could also be attributed to the addition of SiC particles, the poor wettability of which resulted in pores at the particle-matrix interphase as well as lead to low interphase bonding between Al and SiC. Further problem may occur for SiC reinforced Al composites that SiC particles may react with the aluminum at the interphases to form Al<sub>4</sub>C<sub>3</sub> and Si phases along the grain boundary as well as that the surface of the aluminum grains could be covered with thin oxide film that prevent strong bond formation between SiC and aluminum. In either case degradation in the mechanical properties can occur. There are several ways to overcome these problems including the deposition of the SiC particles with thin films possessing good wettability to the alumina melt [13] or alloying the aluminum with Si and Mg [2, 11]. As Al<sub>4</sub>C<sub>3</sub> could not be detected by XRD analysis, it suggests that during the short time of sintering the above mentioned reaction could not take place.

Figures 2.a-c show scanning micrographs of the starting powder mixtures, while Figures 3.a-c compare the fractured surface of the sintered samples. Analyzing the microstructure, SEM images show a considerable difference in the size of the grains of the aluminum matrix and those of the reinforcing particles. It can be also observed that the reinforcing particles remained agglomerated and did not create a homogenous dispersion in the matrix in spite of the intensive milling. This favors a pattern, in which the reinforcing phases situate around the Al grains creating a quasi coherent network.

**Figure 1a-1c.** Sintering curves of experiments 1-3 (a-c)

The images made of the fractured surface of the composite did not reveal the particular pores, but it can be perceived that fracture occurred along the grain boundaries of the additive particles protruding the surface that confirms the poor wettability of the nonmetallic phases.

## Conclusions

Aluminum matrix composites were prepared using various ceramic particles and graphene as reinforcing phases by powder metallurgical method applying novel spark plasma synthesis. The characteristic of the starting material is the nanometer sized reinforcing phases as well as their relatively higher proportions (30-70 wt%) in the matrix. Due to the generally lower temperature and time duration of SPS sintering we managed to avoid the reactions between different phases at the interphase to form Al<sub>4</sub>C<sub>3</sub> that would be a detrimental effect on the mechanical properties.

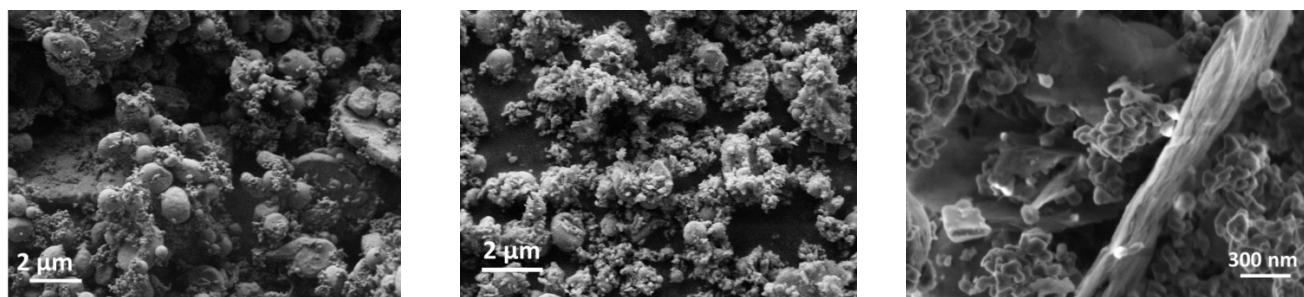


Figure 2a-2c. SEM images of the starting mixture of the particulate experiments

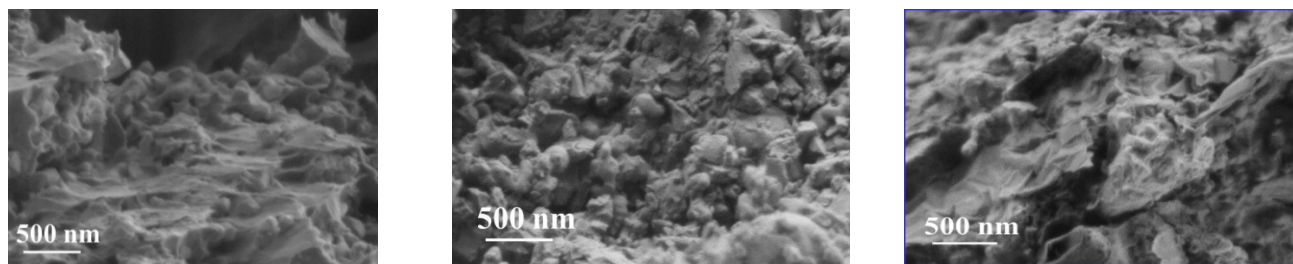


Figure 3a-3c. SEM images of the fractured surface of sintered discs prepared in the particulate experiments

Dense composite with improved hardness, however, could be achieved having the reinforcing phases in the lowest (30 wt. %) proportion in the matrix. Increasing the reinforcing phases the porosity also increased considerably decreasing the hardness. Therefore, it is reasonable to avoid the incorporation of reinforcing particles in higher amount in the matrix or their surface must be deposited previously with a thin film creating good wettability to aluminum. Further research will be conducted in this direction.

### Acknowledgements

This work was supported by the National Office for Research and Technology (NKTH) (Project No: REG-KM-09-1-2009-0005). The authors acknowledge the Hungarian-Indian co-operation R&D&I framework program TET\_09\_IN\_DST (ALNANO09)

### References

- <sup>1</sup>Mahdavi, S., Akhlaghi, F., *Tribol. Lett.*, **2011**, *44*, 1.
- <sup>2</sup>Mazahery, A. and Shabani, M. O., *Strength of Materials*, **2012**, *44*.

- <sup>3</sup>Dash, K., Chaira, D., Ray, B. C., *Mater. Res. Bull.*, **2013**, *48*, 2535.
- <sup>4</sup>Show, B. K., Mondal, D. K., Biswas, K., Maity, J., *Mater. Sci. Eng. A*, **2013**, *579*, 136.
- <sup>5</sup>Ravindran, P., Manisekar, K., Vinoth Kumar, S., Rathika, P., *Mater. Design*. **2013**, *51*, 448.
- <sup>6</sup>Mahdavi, S., Akhlaghi, F., *J. Mater. Sci.*, **2011**, *46*, 7883.
- <sup>7</sup>Lee, Ch., Wei, X., Kysar, J. W., Hone, J., *Science*, **2008**, *321*, 385.
- <sup>8</sup>Porwala, H., Tatarok, P., Grasso, S., Khaliqa, J., Dlouhý, I., Reece, M. J., *Carbon*, **2013**, *64*, 359.
- <sup>9</sup>Jian L., Haixue, Y., Kyle, J., *Ceram. Int.*, **2013**, *39*, 6215.
- <sup>10</sup>Mizuuchi, K., Inoue, K., Agari, Y., Nagaoka, T., Sugioka, M., Tanaka, M., Takeuchi, T., Tani, J., Kawahara, M., Makino, Y., Ito, M., *Composites: Part B*, **2012**, *43*, 2012.
- <sup>11</sup>Bhushan, R. K., Kumar, S., Das, S., *Int. J. Adv. Manuf. Technol.*, **2013**, *65*, 611.
- <sup>12</sup>Kun P., Wéber F., Balázs, C., *Centr. Eur. J. Chem.*, **2011**, *9*, 47.
- <sup>13</sup>Kretz F., Gácsi Z., Kovács J., Pieczonka T., *Surf. Coat Technol.*, **2004**, *180-181*, 575.

Received: 10.01.2014.

Accepted: 24.01.2014.